Leukemia Research 122 (2022) 106949

Contents lists available at ScienceDirect

Leukemia Research

journal homepage: www.elsevier.com/locate/leukres

Research paper

Bortezomib-resistant multiple myeloma patient-derived xenograft is sensitive to anti-CD47 therapy

Yanhua Yue [a,b], Yang Cao [a], Fei Wang [a], Naidong Zhang [b], Ziwei Qi [b], Xunyuan Mao [b], Shuxin Guo [b], Feng Li [a], Yanting Guo [a], Yan Lin [a], Weimin Dong [a], Yuhui Huang [b,*], Weiying Gu [a,**]

[a] Department of Hematology, The First People's Hospital of Changzhou, Third Affiliated Hospital of Soochow University, Changzhou, Jiangsu Province, PR China
[b] Cyrus Tang Hematology Center, Collaborative Innovation Center of Hematology, State Key Laboratory of Radiation Medicine and Prevention, Soochow University, Suzhou, Jiangsu Province, PR China

ARTICLE INFO

Keywords:
Multiple myeloma
Bortezomib-resistance
Anti-CD47 antibody
Tumor-associated macrophages
Angiogenesis

ABSTRACT

Multiple myeloma (MM) remains an incurable hematologic malignancy due to its frequent drug resistance and relapse. Cluster of Differentiation 47 (CD47) is reported to be highly expressed on MM cells, suggesting that the blockade of CD47 signaling pathway could be a potential therapeutic candidate for MM. In this study, we developed a bortezomib-resistant myeloma patient-derived xenograft (PDX) from an extramedullary pleural effusion myeloma patient sample. Notably, anti-CD47 antibody treatments significantly inhibited tumor growth not only in MM cell line-derived models, including MM.1S and NCI-H929, but also in the bortezomib-resistant MM PDX model. Flow cytometric data showed that anti-CD47 therapy promoted the polarization of tumor-associated macrophages from an M2- to an M1-like phenotype. In addition, anti-CD47 therapy decreased the expression of pro-angiogenic factors, increased the expression of anti-angiogenic factors, and improved tumor vascular function, suggesting that anti-CD47 therapy induces tumor vascular normalization. Taken together, these data show that anti-CD47 antibody therapy reconditions the tumor immune microenvironment and inhibits the tumor growth of bortezomib-resistant myeloma PDX. Our findings suggest that CD47 is a potential new target to treat bortezomib-resistant MM.

1. Introduction

Multiple myeloma (MM), the second most common hematological malignancy after lymphoma, is a clonal plasma cell neoplasm in bone marrow [1]. Nowadays the advents of novel treatments, such as proteasome inhibitors, immunomodulatory drugs, monoclonal antibodies, histone deacetylase inhibitors, chimeric antigen receptor T-cell (CAR-T) therapy, and autologous transplantation, have transformed the management of MM patients and improved the outcomes of MM patients. Despite recent therapeutic advances, MM remains to be an incurable disease due to the frequent resistance and relapse. Therefore, new therapies are imperative to target and eradicate resistant myeloma-initiating cells.

Cluster of Differentiation 47 (CD47) is a heavily glycosylated transmembrane protein, which can bind to various proteins including integrin, signal regulatory protein-α (SIRPα), thrombospondin (TSP)-1 and -2 [2]. The interaction of CD47 with SIRPα activates the "don't eat me" signal to the macrophages to inhibit phagocytosis. CD47 is ubiquitously expressed on human healthy cells but overexpressed on many types of tumor cells including hematologic malignancies and solid cancers [3–7]. Cancer cells can identify the "self" signal and promote CD47 expression to upregulate the anti-phagocytic signal. The phagocytosis of target cells by macrophages is regulated by a balance of pro-phagocytic and anti-phagocytic signals [8–11], of which CD47-SIRPα is an important anti-phagocytic signaling pathway. CD47 overexpression in malignancies suppresses macrophages from engulfing

* Correspondence to: Cyrus Tang Hematology Center, Collaborative Innovation Center of Hematology, State Key Laboratory of Radiation Medicine and Prevention, Soochow University, 199 Ren-Ai Road, Suzhou 215123, Jiangsu Province, PR China.
** Correspondence to: Department of Hematology, The First People's Hospital of Changzhou, Third Affiliated Hospital of Soochow University, 185 of Juqian Road, Tianning District, Changzhou 213003, Jiangsu Province, PR China.
E-mail addresses: huangyh@suda.edu.cn (Y. Huang), guweiying2001@163.com (W. Gu).

https://doi.org/10.1016/j.leukres.2022.106949
Received 4 May 2022; Received in revised form 28 August 2022; Accepted 2 September 2022
Available online 6 September 2022

malignant cells, which helps malignant cells to evade immune surveillance. A significant increase of CD47 expression on plasma cells has been identified from the monoclonal gammopathy of undetermined significance (MGUS) to MM [12,13]. Another study revealed that 73% of MM patients had CD47 overexpression compared with non-myeloma cells [14]. Additionally, the progression of MM is directly correlated with CD47 mRNA expression and primary MM cells had a higher CD47 expression compared to other bone marrow cell populations [14–16].

Anti-CD47 antibodies can exert anti-tumor activities in hematologic malignancies and solid tumors even in advanced cancers [17–19]. Several antibodies to block the CD47- SIRPα pathway, like B6H12.2, TTI-621, TTI-622, AO-176 and SRF231, have been studied to treat MM and the preclinical data showed promising results [17,19]. As to the mechanism of anti-CD47 antibodies against tumors, three different points have been raised including the initiation of type III programmed cell death, the blockade of anti-phagocytic signal, and the stimulation of cytotoxic T cells [20–22]. Previous studies have demonstrated that anti-CD47 antibodies could inhibit the growth of MM by the first two of three effect mechanisms. Kikuchi et al. reported that bivalent single-chain antibody fragments against CD47 showed an anti-MM potency through inducing MM cell apoptosis [23]. Subsequent studies revealed that anti-CD47 antibody B6H12.2 or MiR-155 overexpression inhibited human MM growth in mouse models via the engulfment of MM cells by macrophages [14,16]. What's more, Peluso MO et al. demonstrated that the fully human anti-CD47 antibody SRF231 elicits dual-mechanism antitumor activity via inducing apoptosis and phagocytosis involving macrophages [22]. Since these studies have shown that CD47 blockade can exert an anti-MM effect in vitro and in vivo, we hypothesize that anti-CD47 antibody can suppress the growth of resistant MM.

This study reported the therapeutic effects of fully human anti-CD47 antibody IBI188 on MM and explored its possible influences on the tumor microenvironment in the mouse models. We found that anti-CD47 antibody exerts a potent anti-MM activity regardless of bortezomib (BTZ)-resistance. Further studies demonstrate that anti-CD47 antibody therapy optimizes the subpopulation composition of tumor-associated macrophages (TAMs) and normalizes tumor vascular function to improve the tumor microenvironment. Therefore, our work provides the proof-of-concept for clinical evaluation of anti-CD47 antibody in the treatment of BTZ-resistant MM.

2. Materials and methods

2.1. Cell lines, human samples and reagents

Human MM cell lines MM.1S and NCI-H929 were obtained from the American Type Culture Collection (Manassas, VA, USA), which were authenticated by short-tandem repeat profiling and were routinely tested negative for mycoplasma contamination. Cells were cultured in complete RPMI 1640 medium including 100 IU/ml penicillin, 100 μg/ml streptomycin, and 10% fetal bovine serum (Hyclone) at 37 °C in 5% CO_2 atmosphere in a humidified chamber. Bone marrow (BM) cells from healthy donors and pleural effusion cells from one MM patient were collected after written informed consent and the institutional ethics committee approval by The Third Affiliated Hospital of Soochow University. According to the International Myeloma Working Group, diagnosis and relapse of MM were defined [24]. The pleural effusion sample of extramedullary myeloma came from one patient with relapsed and resistant IgD-lambda type MM. The characteristics of the MM patient was shown in Table 1. Mononuclear cells (MNCs) were isolated from pleural effusion and bone marrow samples using Ficoll-Hypaque (Sigma-Aldrich).

Recombinant fully human IgG4 anti-CD47 monoclonal antibody (IBI188), a gift from Innovent Biologics Pharmaceutical Co., Ltd. (Suzhou, China), is provided at a concentration of 90–110 mg/ml. An isotype-matched control human antibody IgG was purchased from suppliers. Anti-CD47 monoclonal antibody and IgG were diluted in Dulbecco's phosphate-buffered saline (PBS, Gibco) before in vivo administration. BTZ was presented from Jiangsu Chia-Tai Tianqing Pharmaceutical Co, Ltd (Nanjing, China). BTZ was firstly dissolved in Dimethyl Sulfoxide (Sigma-Aldrich) and then was diluted by double distilled water (ddH2O).

2.2. Patient-derived xenograft models

Female *NOD.CB17-Prkdc^{scid} Il2rg^{tm1}/Bcgen* (*B-NDG*) mice (5–6 weeks old) were purchased from BIOCYTOGEN (Beijing, China). Mice were bred in the specific pathogen-free (SPF) condition at Soochow University. MM.1S cells (2×10^6 cells), NCI-H929 cells (2×10^6 cells), or MNCs (1×10^7 cells) from MM patient were mixed with 50 % matrigel (BD Biosciences) and then subcutaneously inoculated into the flank of *NDG* mice. One bortezomib-resistant MM patient-derived xenograft (PDX) was successfully established. When tumors reached 6–8 mm in diameter, tumor tissues in PDX models were isolated and parts of them were transplanted into other *NDG* mice, the rest of them were prepared for Giemsa staining, immunohistochemical (IHC) analysis, and quantitative real-time PCR (qPCR). In BTZ treatment experiments, when tumors reached 4–6 mm in diameter, tumor-bearing mice were randomly divided into bortezomib or control groups. Then mice were administered with 0.5 mg/kg BTZ or vehicle intraperitoneally twice a week for 12 or 15 days. In anti-CD47 antibody treatment experiments, when tumors reached 6–8 mm in diameter, tumor-bearing mice were randomly divided into anti-CD47 or IgG groups. Then mice were administered with anti-CD47 antibody or IgG (100 ug/mouse) every two days for 6 or 9 days by intraperitoneal injection. The size of the tumor was measured every 3 days, and the tumor volume was estimated by the formula [length × width^2 /2]. When mice were euthanized, tumor tissues were isolated, weighed and prepared for flow cytometric analysis, tumor vessel analysis, and qPCR. In the experiment of survival analysis, tumor-bearing mice were euthanized when tumor volume reached 1300 mm^3.

Table 1
The clinical and laboratory characteristics of MM patient.

Age (years)	sex	Disease stage	DS	R-ISS	Type	Treatments	Cytogenetics/FISH	Bone marrow biopsy and immunohistochemistry	Bone marrow cell morphology	Flow cytometry of bone marrow cells
71	M	Relapse	IIIB	III	IgD-lambda	VD * 4, VTD * 4, VCD * 2, IAD * 2,	1q21 amplification (40 %); the deletion of Rb1 (40 %), the deletion of 13q14 (44 %), IgH rearrangement (30 %)	Pleural effusion pathology: small heterotypic cells. Immunohistochemical staining of abnormal plasma cells:AE1/AE3-, CD20-, CD79a-, CD38 + , CR-.	Plasma cell rate 19 % (diagnosis) and 35 % (relapse).	16.5 % of bone marrow nucleated cells were a clonal plasma cell population and positively expressed CD138, CD38 and cLambda.

IAD: ixazomib + liposomal doxorubicin + dexamethasone; M: male; VCD: bortezomib + cyclophosphamide + dexamethasone; VD: bortezomib + dexamethasone; VTD: bortezomib + thalidomide + dexamethasone.

2.3. qPCR

Total RNA from healthy bone marrow cells, MM cells, and tumor tissues in MM mouse models was extracted using a MicroElute Total RNA kit (Omega). Then cDNA was synthesized using a RevertAid First Strand cDNA Synthesis Kit (ThermoFisher Scientific). The qPCR was performed in a High Throughput Quantitative PCR Light Cycler480 (Roche) with Light Cycler 480 SYBR Green I Master mix and primers (Table 2). To reduce nonspecific amplification, one half of the primer was designed to hybridize to the 3′ end of one exon, and the other half hybridized to the 5′ end of the adjacent exon. The examined genes included β-actin, human CD47 and mouse, angiogenesis-related factors, such as vascular endothelial growth factor-α (VEGFα), placental growth factor (PlGF), fibroblast growth factor-1 (FGF1), platelet derived growth factor-α (PDGFα), platelet derived growth factor-D (PDGFD), angiopoietin-2 (Ang2), nitric oxide synthase-2 (NOS2), interleukin-6 (IL6), interleukin-1β (IL1β), angiopoietin-1 (Ang1), thrombospondin-1 (TSP1), platelet factor 4 (PF4), tumor necrosis factor-α (TNFα), interferon-γ (IFNγ), and matrix metalloproteinase-2/9/14 (MMP2/9/14). The relative expression levels of genes were normalized to β-actin and showed by the $2^{-\Delta\Delta Ct}$.

2.4. Flow cytometric analysis

Tumor-bearing mice after treatments were euthanized and immediately perfused via intracardiac injection with PBS. Then, tumor tissues were removed, minced, and digested at 37°C for 45 min with cell detach solution consisting of RPMI 1640, collagenase type 1A (1.5 mg/ml), hyaluronidase (1.5 mg/ml), and DNase (20 U/ml). The digested mixtures were ground and filtered with 70-μm cell strainers. The single-cell suspension was blocked with a rat anti-mouse CD16/CD32 antibody (BD Pharmingen) and then stained with the following mouse fluorochrome-conjugated antibodies: CD45-BV421 (catalog103134, clone 30-F11), CD11b-BV510 (catalog 101263, clone M1/70), Ly-6G-FITC (catalog 551460, clone 1A8), Gr1-APC-Cy7(catalog 47-5931-82, clone RB6-8C5), F4/80-PE (catalog 12-4801-82, clone BM8), CD11c-PE-Cy7 (catalog 25-0114-82, clone N418), and CD206-APC (catalog 141708, clone C068C2). 7-amino-actinomycin D (7AAD, eBioscience) was used for dead cell exclusion. Doublet cells were excluded using side scatter area versus side scatter width. A Gallios flow cytometer (Beckman) was used to examine all of the samples and Kaluza software (version1.3) was used to analyze the data.

Table 2
Primers used in qPCR.

*hβ-actin-Forward	TCATGAAGTGTGACGTGGACATC
hβ-actin-Reverse	CAGGAGGAGCAATGATCTTGATCT
hCD47-Forward	TATCCTCGCTGTGGTTGGAC
hCD47-Reverse	TCATTCCTTTTGATTCTTTGAATGC
*mβ-actin-Forward	ATCGTGCGTGACATCAAAGA
mβ-actin-Reverse	ACAGGATTCCATACCCAAGAAG
mPDGFD-Forward	ATCCGGACACTTTTGCGACT
mPDGFD- Reverse	CCTGAATGTTCTCCTCTCTCTGG
mAng2-Forward	TACAAAGAGGGCTTCGGGAG
mAng2-Reverse	GTTGGACTCTTCACCAGCGA
mPlGF-Forward	ATTCAGTCCGTCCTGTGTCC
mPlGF-Reverse	GGTTTTCCTCCTTTCTGCCT
mPDGFα-Forward	GGAGGAGACAGATGTGAGGTG
mPDGFα-Reverse	GGAGGAGAACAAAGACCGCA
mVEGFα-Forward	AGTCCCATGAAGTGATCAAGTTCA
mVEGFα-Reverse	ATCCGCATGATCTGCATGG
mFGF1-Forward	CCAGCCTGCCAGTTCTTC
mFGF1-Reverse	GGCTGCGAAGGTTGTGAT
mNOS2-Forward	CCACCTCTATCAGGAAGAAA
mNOS2-Reverse	CTGCACCGAAGATATCTTCA
mIL6-Forward	AAATGAGAAAAGAGTTGTGCAATGG
mIL6-Reverse	ATCTCTCTGAAGGACTCTGGCT
mAng1-Forward	ATGGAAAATTATACTCAGTGGCTGC
mAng1-Reverse	ATTTAGTACCTGGGTCTCAACATC
mTNFα-Forward	CCGATGGGTTGTACCTTGTC
mTNFα-Reverse	CGGACTCCGCAAAGTCTAAG
mIFNγ-Forward	CCAAGTTTGAGGTCAACAACCC
mIFNγ-Reverse	GGGACAATCTCTTCCCCACC
mMMP2-Forward	CTGGTGCTCCACCACATACA
mMMP2-Reverse	CACAGTGGACATAGCGGTCT
mMMP9-Forward	CGTGTCTGGAGATTCGACTTGA
mMMP9-Reverse	TTGGAAACTCACACGCCAGA
mMMP14-Forward	ATGGCCCCCTTTTACCAGTG
mMMP14-Reverse	GTGACCCTGACTTGCTTCCATA
mIL1β-Forward	TGCCACCTTTTGACAGTGATG
mIL1β-Reverse	AAGGTCCACGGGAAAGACAC
mPF4-Forward	AGCTCATAGCCACCCTGAAGA
mPF4-Reverse	ACAATTGACATTTAGGCAGCTGAT
mTSP1-Forward	TGTCACTGCCAGAACTCGGTTA
mTSP1-Reverse	GGAGACCAGCCATCGTCAG

* h: human; m: mouse.

2.5. Immunohistochemistry analysis

Tumor blood vessel staining was performed as previously described [25]. Briefly, 5 min after intravenous injection of Hoechst 33342 (10 mg/kg in 200 μl PBS), mice were systemically perfused with PBS, and tumors were isolated and fixed with 4% paraformaldehyde for 3 h, followed by incubation with 30% sucrose overnight. The tissues were OCT-embedded and conserved at − 80 °C. Staining for the endothelial marker CD31 (1:100, clone MEC13.3, catalog 550274, BD Biosciences) was done on frozen sections (20 μm thickness), followed by staining with secondary antibody Alexa Fluor 647 donkey anti-rat IgG (catalog 712-605-153) in dark, humid chambers at room temperature. Fluorescent images were obtained with an Olympus FV3000 confocal laser-scanning microscope. The vessel density and tissue area stained with Ho33342 were assessed by using ImagePro Plus software (version 6.0). The variables were determined for 5 photographic areas from each tumor. Confocal images were taken in randomly selected fields (5 fields per tumor).

2.6. Statistics

Statistical analysis was conducted using Prism software (version 7, GraphPad). All comparisons between two groups were analyzed with unpaired two-tailed Student's *t* tests. Kaplan-Meier and log-rank test were utilized in the survival analysis. All of the data were presented as the mean ± standard error of the mean (SEM). The results were considered statistically significant when $P < 0.05$.

3. Results

3.1. A BTZ-resistant MM PDX expresses a high level of CD47

PDXs have emerged as a useful platform to develop new treatment strategies for MM. In this study, a BTZ-resistant MM PDX in *NDG* mice was successfully generated by subcutaneous inoculation of MNCs from pleural effusion of one relapsed and resistant MM patient, following series tumor tissue transplantation (Fig. 1a). Next, we investigated the characteristics of tumors in the MM PDX by morphological and phenotypic analysis. The Giemsa staining showed that tumor cells from the MM PDX presented a malformed plasma cell morphology with eccentric nuclei (Fig. 1b). IHC staining revealed that tumor cells in the PDX expressed CD138, CD38, and light chain lambda without light chain kappa expression, and 70 % of tumor cells expressed Ki-67 (Fig. 1c). Therefore, the PDX exhibited the phenotype of $CD138^{+}$ malignant plasma cells with the restrictive expression of lambda. Furthermore, we verified whether the PDX model retained primary drug sensitivity as seen in the clinic. Since the PDX model was derived from a MM patient with resistance to BTZ, we intraperitoneally administered BTZ with a dose of 0.5 mg/kg twice a week according to previous studies in this model [26,27]. After 4–5 doses of BTZ treatments, the tumor growth curve of MM PDX in the BTZ group was similar to that in the control

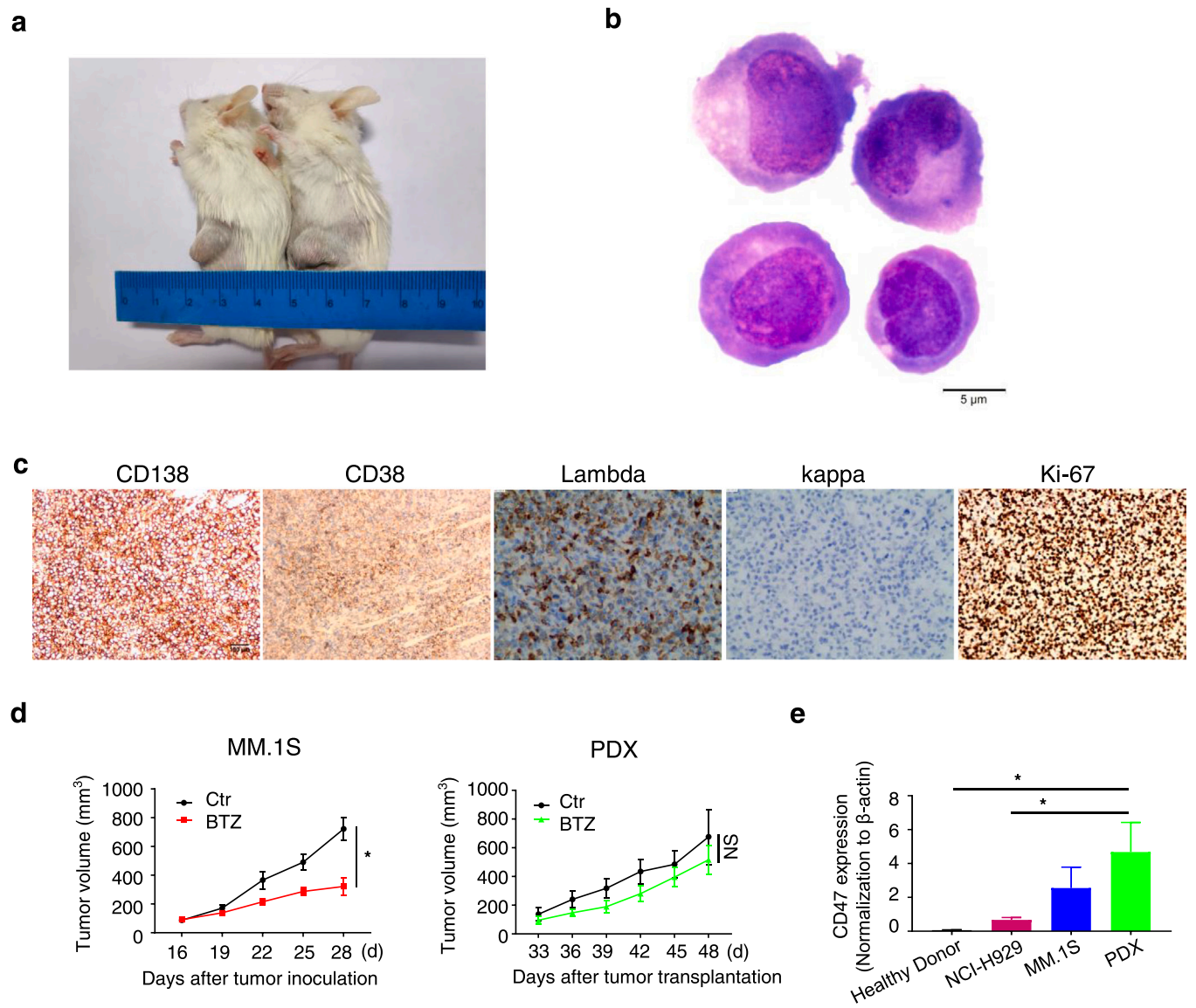

Fig. 1. The characteristics of tumor cells from a BTZ-resistant MM PDX. Primary MM cells isolated from a pleural effusion sample or MM.1S cells were subcutaneously inoculated in *NDG* mice. When tumors grew to 6–8 mm in diameter, PDX tumor tissues were isolated and parts of them were implanted into the recipient mice, the others were prepared for single-cell suspension and IHC staining. (a) A representative image of MM PDX. (b) Giemsa staining showed the morphology of tumor cells from the MM PDX. Scale bar: 5 μm. (c) Representative IHC staining of tumor tissues. Scale bar: 100 μm. (d) When tumors reached 4–6 mm in diameter, mice were randomly divided into two groups respectively in MM.1S and PDX models. BTZ therapy: tumor-bearing mice (n = 4–5 every group) were intraperitoneally administered with BTZ (0.5 mg/kg) every Monday and Thursday for a total of 5 doses, and the control group was treated with phosphate-buffered saline (PBS). Tumor size was measured every three days. (e) CD47 expression on healthy bone marrow cells, MM cell lines and MM PDX cells by qPCR. MM: multiple myeloma. PDX: patient-derived xenograft. IHC staining: immunohistochemical staining. Ctr: control group. BTZ: BTZ treatment group. qPCR: quantitative real-time PCR. Data were from one experiment representative of two independent experiments with similar results. Data were shown as mean ± SEM. Significance was determined by unpaired two-tailed Student's *t*-test. *NS: no significance,* * $P < 0.05$.

group, while MM.1S tumor growth curves have a significant difference between the BTZ group and vehicle control group (Fig. 1d). Therefore, the MM PDX preserves its primary drug resistance to BTZ. Several studies have reported that MM patients highly expressed CD47 [12,14,15]. To determine the level of CD47 expression in the MM PDX, we performed qPCR in healthy bone marrow cells, myeloma cell lines, and tumor cells from the PDX. The result showed that the MM PDX expressed a higher level of CD47 compared with healthy bone marrow cells and NCI-H929 cells, while MM.1S cells expressed the intermediate level of CD47 between MM PDX and healthy donors (Fig. 1e). Together, we develop a practical approach to establish MM PDX and show that a BTZ-resistant MM PDX highly expresses CD47.

3.2. *Anti-CD47 treatments inhibit the growth of both MM cell line-derived and BTZ-resistant PDX tumors*

Previous studies showed that anti-CD47 antibodies B6H12.2 and SRF231 can inhibit the growth of human RPMI 8226, OPM-2, and patient myeloma cells in mouse xenotransplantation models [14,22]. Thus, we investigated the treatment effect of anti-CD47 antibody IBI188 in MM mouse models. Firstly, we treated MM.1S and NCI-H929 tumor-bearing mice with anti-CD47 antibody every two days for 6 or 9 days (Fig. 2a). The inhibition rates of tumor growth upon anti-CD47 antibody treatments were 86.68% and 78.62% in MM.1S and NCI-H929 myeloma mouse models, respectively (Fig. 2b). These data suggested that both of MM.1S and NCI-H929 myeloma cells were sensitive to anti-CD47

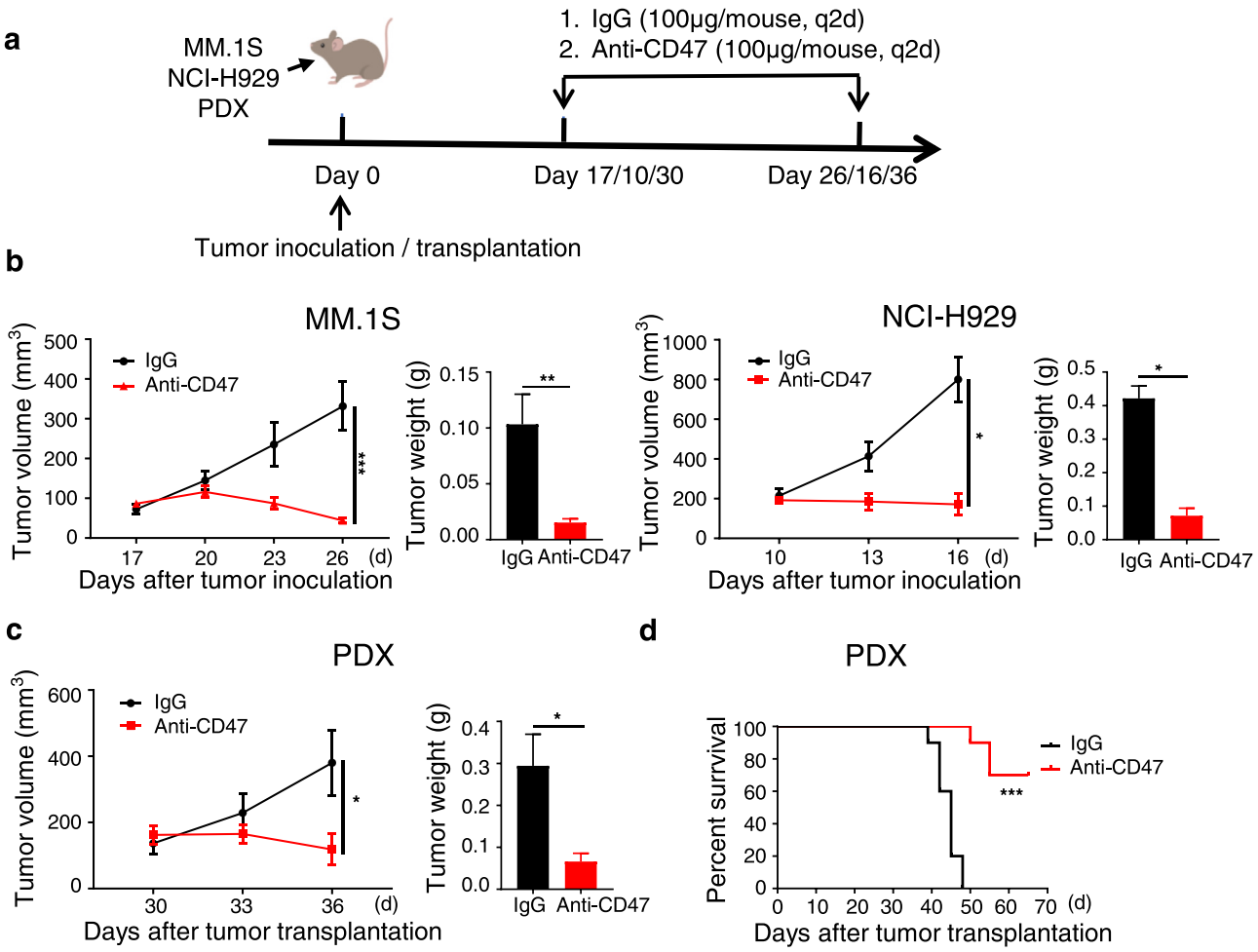

Fig. 2. Anti-CD47 therapy suppressed the growth of MM cell line-derived and bortezomib-resistant PDX tumors. (a) Experimental design: *NDG* mice were subcutaneously inoculated or implanted with MM.1S, NCI-H929 MM cells and tumor pieces (1–2 mm^3) of BTZ-resistant PDX on the flank. When tumors reached 6–8 mm in diameter, mice were randomly divided into two groups in every model. Anti-CD47 therapy: tumor-bearing mice (n = 6–7 every group) received anti-CD47 antibody (100 μg /mouse) every two days for 6 or 9 days by intraperitoneal injection, and the control group was treated with IgG. (b and c) Tumor size was measured every three days, and tumor weight was measured at the end of the treatment. Significance was determined by unpaired two-tailed Student's *t*-test. (d) The survival of BTZ-resistant PDX tumor-bearing mice treated with IgG or anti-CD47 antibody (n = 10 every group). Mice were euthanized when tumors reached 1300 mm^3. The survival of mice was calculated by Kaplan-Meier analysis ($P < 0.001$, log rank test). MM: multiple myeloma. PDX: patient-derived xenograft. IgG: control group. Anti-CD47: anti-CD47 antibody treatment group. Data were from one experiment representative of two independent experiments with similar results. Data were shown as mean ± SEM. * $P < 0.05$, * * $P < 0.01$, * ** $P < 0.001$.

antibody. Next, to determine whether anti-CD47 antibody can overcome BTZ-resistance, we administered anti-CD47 antibody in our BTZ-resistant MM PDX (Fig. 2a). The results showed that the BTZ-resistant MM PDX was sensitive to anti-CD47 antibody and the myeloma inhibition rate was 68.84% (Fig. 2c). Further Kaplan-Meier analysis revealed that anti-CD47 treatments significantly extended the survival of BTZ-resistant MM PDX mice compared with the control group (Fig. 2d). Thus, anti-CD47 antibody treatments exert a potent anti-MM effect even in BTZ-resistant MM.

3.3. Anti-CD47 treatments increase the percentage of tumor-associated macrophages (TAMs) and polarize TAMs toward an M1-like phenotype

The immune checkpoint CD47-SIRPα pathway is bound up with macrophages in the tumor microenvironment. SIRPα is abundantly expressed on macrophages, dendritic cells, neutrophils, and neurons [28]. It has been reported that the phagocytosis of myeloma cells by macrophages is enhanced by the blockade of CD47-SIRPα signaling pathway [14]. Next, we studied how anti-CD47 treatments influenced tumor immune microenvironment of MM in *NDG* mouse models. The composition of tumor-associated myeloid cells was analyzed after IgG or anti-CD47 antibody treatments by flow cytometry. The results showed that anti-CD47 treatments elevated the proportion of TAMs ($CD45^+CD11b^+Gr1^-F4/80^+$) in the PDX and MM.1S models (Fig. 3a). The plasticity of TAMs is presented as a continuum of phenotypes, of which M1-like and M2-like TAMs are on behalf of two extreme states [29]. The makers of CD11c and CD206 are generally applied to identify M1- and M2-like TAMs [29,30]. $CD11c^-CD206^-$ ($CD45^+CD11b^+Gr1^-F4/80^+CD11c^-CD206^-$) TAMs and $CD11c^+CD206^+$ ($CD45^+CD11b^+Gr1^-F4/80^+CD11c^+CD206^+$) TAMs represent two populations of intermediate differentiation states. The macrophage subpopulation analysis indicated that M1-like ($CD45^+CD11b^+Gr1^-F4/80^+CD11c^+CD206^-$) TAMs and $CD11c^-CD206^-$ TAMs were increased while M2-like ($CD45^+CD11b^+Gr1^-F4/80^+CD11c^-CD206^+$) TAMs and $CD11c^+CD206^+$ TAMs were decreased after anti-CD47 antibody therapy in the PDX and MM.1S models (Fig. 3b). These data show that anti-CD47 therapy increases the accumulation of antitumoral M1-like TAMs in MM.

3.4. Anti-CD47 treatments induce tumor vascular normalization in MM

TAMs population is one of the major contributors to the process of tumor angiogenesis [31]. The M1-like and M2-like subsets possess

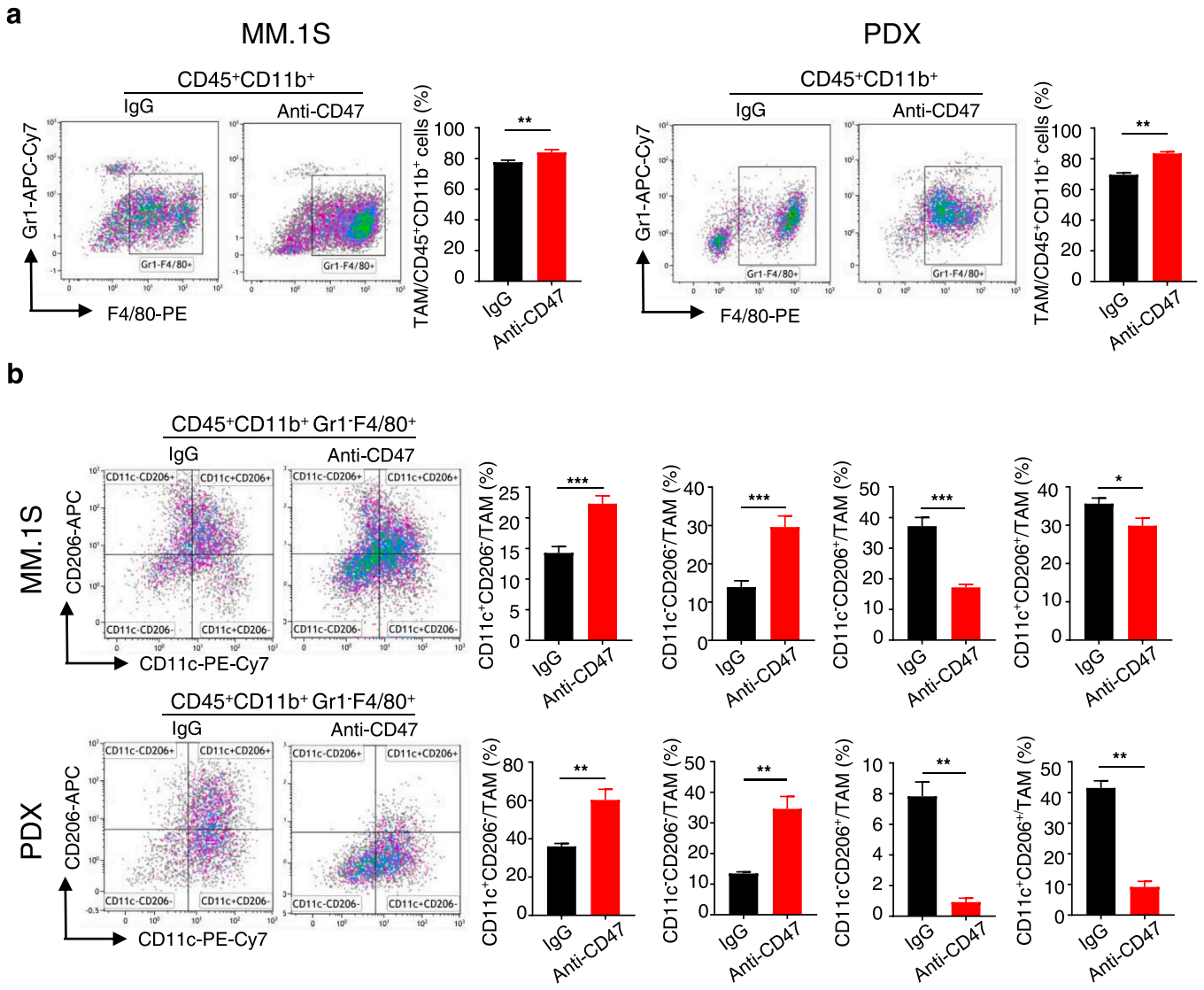

Fig. 3. CD47 blockade increased the proportion of tumor-associated macrophages (TAMs) and polarized TAMs toward an M1-like phenotype in myeloma tumors. Tumor-bearing *NDG* mice were prepared and treated with IgG or anti-CD47 antibody as described in Fig. 2. Tumors were excised and single cell suspensions were prepared for flow cytometry. The aggregated events and dead cells were gated out. (a) The proportion of TAMs in MM.1S and PDX myeloma models. (b) The proportions of TAM subsets in MM.1S and PDX myeloma models. TAMs: $CD45^+CD11b^+Gr1^-F4/80^+$ cells, $CD11c^+CD206^-$: $CD45^+CD11b^+Gr1^-F4/80^+CD11c^+CD206^-$ cells, $CD11c^-CD206^-$: $CD45^+CD11b^+Gr1^-F4/80^+CD11c^-CD206^-$ cells, $CD11c^-CD206^+$: $CD45^+CD11b^+Gr1^-F4/80^+CD11c^-CD206^+$ cells, $CD11c^+CD206^+$: $CD45^+CD11b^+Gr1^-F4/80^+CD11c^+CD206^+$ cells. MM: multiple myeloma. PDX: patient-derived xenograft. IgG: control group. Anti-CD47: anti-CD47 antibody treatment group. Significance was determined by unpaired two-tailed Student's *t*-test. Data were from one experiment representative of two independent experiments with similar results. All data were presented as means ± SEM. * $P < 0.05$, * * $P < 0.01$, * ** $P < 0.001$.

different angiogenic properties [32]. Tumor angiogenesis is a hallmark of MM [33]. Next, we investigated the effects of anti-CD47 antibody treatments on tumor vessel density and perfusion in MM mouse models. Mice were intravenously injected with Ho33342, then Ho33342 circulated for 5 min before tumor harvest. The area of Ho33342 represents tumor vessel perfusion. In both the PDX and MM.1S models, tumor vessel density decreased while tumor vessel perfusion did not decrease and the ratio of tumor vessel perfusion and density increased in anti-CD47 antibody treatment groups compared with control groups, which suggested that tumor vascular permeability was reduced and tumor blood vessel was normalized after anti-CD47 antibody treatments (Fig. 4a and b). These data suggest that anti-CD47 therapy induces tumor vascular normalization in MM.

3.5. Anti-CD47 treatments decrease the expression of pro-angiogenic factors while increase the expression of anti-angiogenic factors in MM

To further explore how anti-CD47 antibody treatments normalize tumor blood vessels in MM, we analyzed the expression of angiogenesis-related genes by qPCR in the MM.1S and PDX models. The results showed that pro-angiogenic genes, including VEGFα, PDGFα, PDGFD, Ang2, and PlGF, were down-regulated while angiostatic genes, including TSP1, PF4, and IFNγ, were up-regulated in anti-CD47-treated groups of MM.1S and PDX models compared to control groups (Fig. 5a and b). These data show that anti-CD47 antibody therapy in MM reduces the expression of pro-angiogenic factors while elevates the expression of angiostatic factors.

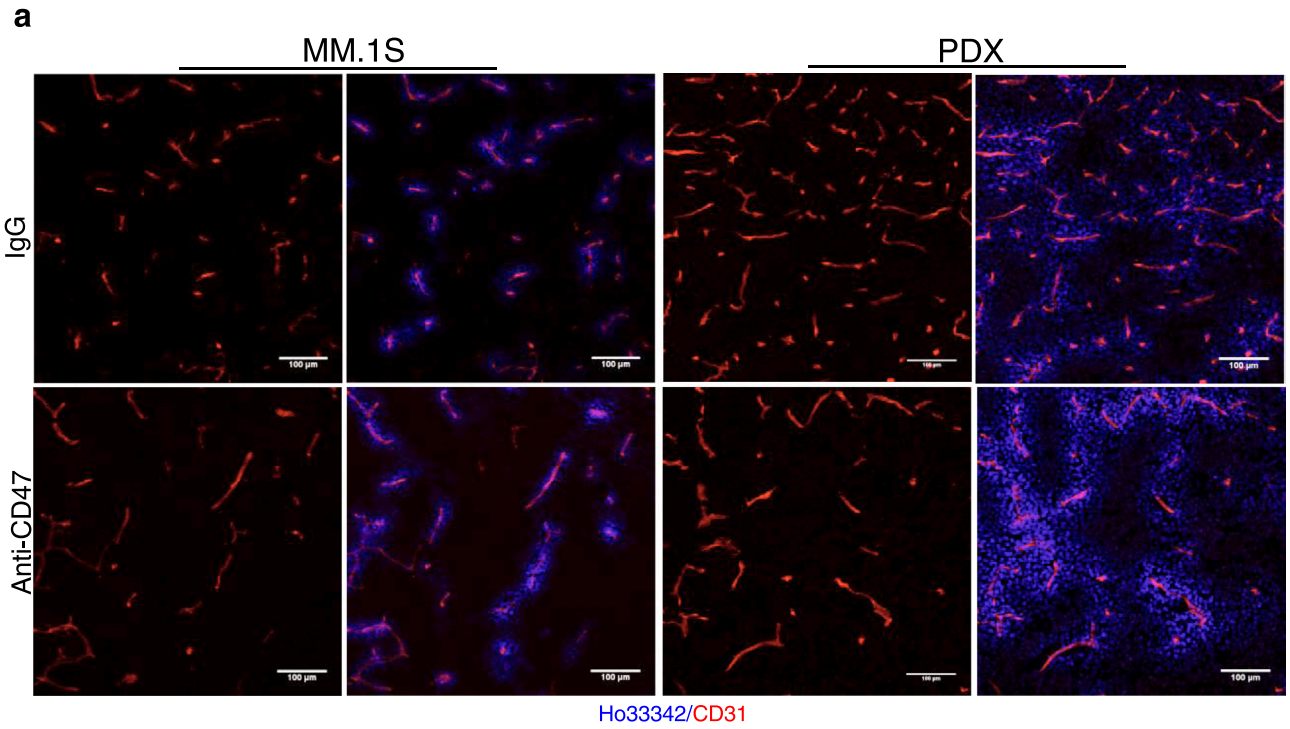

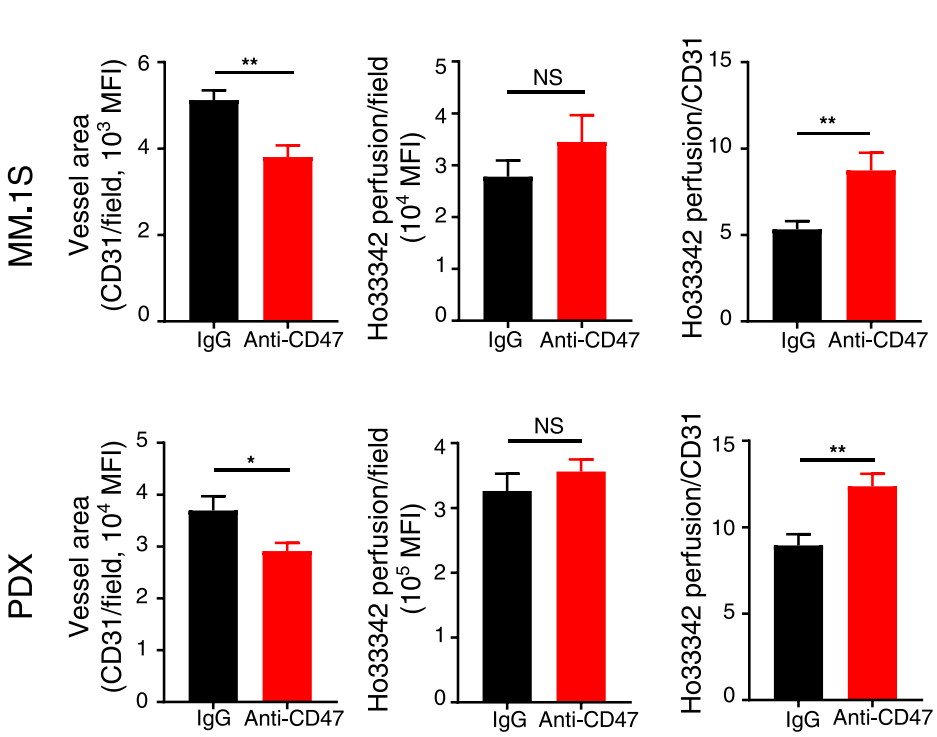

Fig. 4. Anti-CD47 therapy in MM induced tumor vascular normalization. Tumor-bearing *NDG* mice were administrated as described in Fig. 2. Mice were injected with 200 μg Ho33342 five minutes before tumor harvest. Then tumor tissues were stained with anti-CD31 antibody. (a) Representative images indicated tumor vessel density (red) and tumor vessel perfusion (blue) in MM.1S and PDX myeloma models. Scale bar: 100 μm. (b) Quantification of tumor vessel density and tumor vessel perfusion. MM: multiple myeloma. PDX: patient-derived xenograft. MFI: mean fluorescence intensity. CD31: an endothelial cell marker. The intensity of Ho33342 perfusion represents tumor vessel perfusion. The ratio of Ho33342 perfusion and CD31 reflects tumor blood vessel function. IgG: control group. Anti-CD47: anti-CD47 antibody treatment group. Data were from one experiment representative of two independent experiments with similar results. Data were shown as mean ± SEM. Significance was determined by unpaired two-tailed Student's *t*-test. *NS: no significance,* * $P < 0.05$, * * $P < 0.01$.

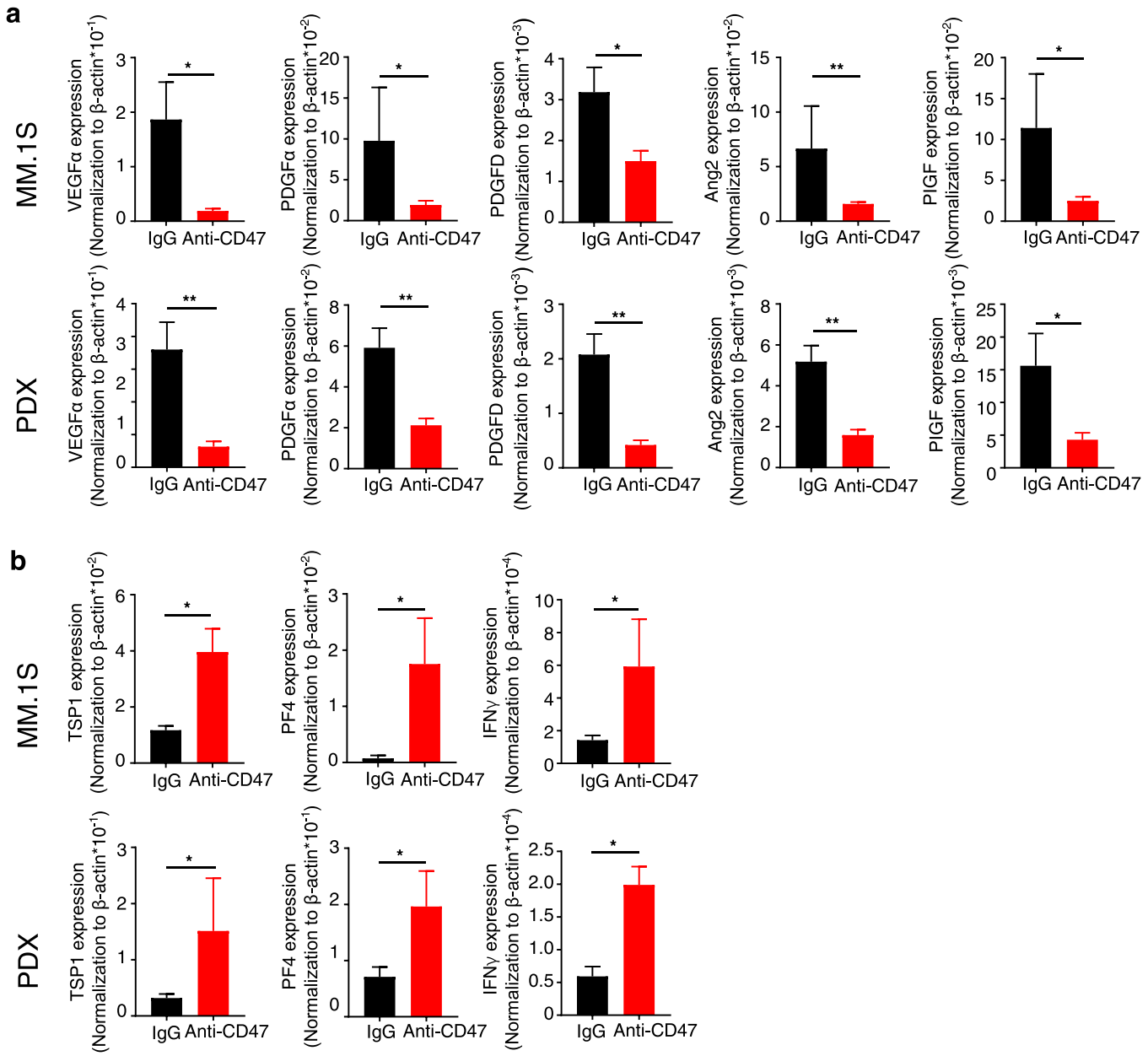

Fig. 5. Anti-CD47 treatments in MM reduced the expression of pro-angiogenic factors while increased the expression of angiostatic factors. Tumor-bearing *NDG* mice were administrated as described in Fig. 2. Then tumor tissues were collected and total RNA was isolated from tumor tissues in MM.1S and PDX myeloma models. (a) The expression of pro-angiogenic genes was identified by qPCR. (b) The expression of anti-angiogenic genes was examined by qPCR. qPCR: quantitative real-time PCR. MM: multiple myeloma. PDX: patient-derived xenograft. IgG: control group. Anti-CD47: anti-CD47 antibody treatment group. Data were from one experiment representative of two independent experiments with similar results. Data were shown as mean ± SEM. Significance was determined by unpaired two-tailed Student's *t*-test. * $P < 0.05$, * * $P < 0.01$.

4. Discussion

Despite the approval of novel agents that improved the depth and duration of the treatment response, MM is incurable due to the eventual emergence of resistance and imminent relapse [34]. Long-term survival remains dismal with no more than 10–15% of transplant patients, and even fewer transplant-unavailable patients were cured [35]. CD47-SIRPα immune checkpoint pathway is upregulated in the majority of MM patients. Several clinical trials (NCT03530683, NCT04445701, NCT03512340, and NCT02663518) are currently underway to inhibit CD47-SIRPα signaling pathway as monotherapy or in combination with other drugs in MM. A phase I study (NCT02663518) shows that the CD47 blocker TTI-621 is well-tolerated and takes effect as monotherapy in patients with relapsed/refractory B-cell non-Hodgkin lymphoma (NHL) and T-cell NHL [36]. However, whether the blockade of CD47-SIRPα signaling pathway can exert an anti-MM role in resistant MM remains unknown. This study established a BTZ-resistant MM PDX and demonstrated that anti-CD47 antibody therapy inhibited the growth of BTZ-resistant myeloma. Moreover, anti-CD47 antibody therapy in MM boosted the accumulation of M1-like macrophages and improved tumor vascular function. Therefore, anti-CD47 antibody can overcome BTZ resistance and exert a potent anti-MM activity.

Since patient-derived MM cells are difficult to propagate in mouse models, in recent years, a zebrafish xenograft model has been reported that permits rapid growth of human MM cells and can be used to assess drug sensitivity or resistance [37]. This study generated a BTZ-resistant MM PDX mouse model from MNCs of extramedullary pleural effusion. The tumor cells from the PDX maintained the essential morphological

and phenotypic characteristics of MM cells. Although this MM PDX mouse model did not present typical symptoms such as bone destruction, hypercalcemia, anemia and renal insufficiency, it reserved primary drug sensitivity and can be used to investigate new therapies. Hence, this PDX is a novel preclinical MM model. In the future, we will collect more intramedullary and extramedullary samples of MM patients to establish MM PDX in order to further validate and improve this modeling approach. We used the MM PDX to discover the potential of anti-CD47 antibody to overcome BTZ resistance. Furthermore, the expression level of CD47 does not seem to be a predictive factor of anti-CD47 treatment response, as suggested by the response in our MM mouse models.

TAMs are an important component in the BM of MM patients, constituting approximately 10% of the BM [38]. BM neovascularization in MM promotes disease progression, and more evidence has suggested that TAMs in the BM microenvironment play a role through angiogenic and vasculogenic activities [39]. Previous studies indicated that the pro-angiogenic TAMs present an M2-like phenotype rather than M1-like TAMs [40]. Anti-CD47 treatments in MM mouse models increased the percentage of TAMs and polarize TAMs from an M2- to M1-like phenotype. Accordingly, anti-CD47 antibody treatments reduce the pro-angiogenic M2-like TAMs, which may result in compromised myeloma angiogenesis. Our data further revealed that anti-CD47 antibody treatments normalized myeloma vascular function. If the treatment facilitates tumor vascular normalization, the ratio of tumor vessel perfusion and tumor vessel density could be improved when tumor vessel density decreases [41]. In both MM.1S and PDX models, anti-CD47 treatments significantly increased the ratio of tumor vessel perfusion and tumor vessel density, which suggested that anti-CD47 treatments induced tumor vascular normalization and improved tumor vascular function.

Tumor angiogenesis and tumor blood vessel function are tightly regulated by pro- and anti-angiogenic factors. Bone marrow stromal cells and plasma cells in MM produce important pro-angiogenic factors, such as VEGF, FGFβ, transforming growth factor β (TGFβ), and interleukin-8 (IL-8), to stimulate angiogenesis [42,43]. Anti-CD47 therapy in MM downregulates pro-angiogenic gene expression, like VEGFα, PDGFα, PDGFD, Ang2, and PlGF, and upregulates anti-angiogenic gene expression, like TSP1, PF4, and IFNγ, which rebalances pro- and anti-angiogenic factors. Among these factors, VEGF, PDGF, and PlGF can be secreted by M2-like TAMs, which foster tumor angiogenesis to accelerate tumorigenesis, progression, and recurrence [44,45]. Ang2, a potent inducer of angiogenesis, vascular destabilization, and vascular permeability, interacts with Tie2-expressing macrophages to facilitate angiogenesis and tumorigenesis in mammary carcinomas and pancreatic insulinomas [46,47]. Besides, TSP1 and PF4 are intrinsic angiostatic factors [48,49], while IFNγ is an immune effector molecule with potent angiostatic activity [44,50]. Therefore, the improved balance of pro- and anti-angiogenic factors by anti-CD47 antibody therapy may induce tumor blood vessel normalization, and the polarization of TAMs from M2- to M1-like subset might reduce pro-angiogenic factors secretion. Earlier researches of tumor vascular normalization mainly focused on the VEGF-VEGFR axis, recent studies have revealed the Ang-Ang1 receptor (Tie2) signaling pathway as a novel target for normalizing tumor vessels [47]. However, further studies are needed to elucidate the underlying molecular mechanism of how anti-CD47 therapy induces tumor vascular normalization in MM.

Tumor blood vessel normalization contributes to the improvement of the tumor microenvironment and promotes the delivery of antineoplastic drugs into tumors. Therefore, CD47-targeted therapy might exert anti-MM activity partially by restoring the normal function of blood vessel. Although it is widely believed that anti-CD47 therapy exerts an anti-tumor activity through the engulfment of tumor cells by macrophages, the immune-vascular crosstalk may also influence the effect of anti-CD47 antibody in tumors.

5. Conclusion

Anti-CD47 antibody treatments suppress tumor growth in MM mouse models even the BTZ -resistant PDX. Furthermore, CD47 blockade in MM increases the proportion of TAMs and promotes the polarization of M2- to M1-like TAMs. Strikingly, anti-CD47 therapy modifies the balance of pro-angiogenic and anti-angiogenic gene expression and normalizes myeloma blood vessel function. Taken together, anti-CD47 treatments improve the tumor microenvironment of MM to exert an anti-MM effect. Therefore, this study demonstrates the potential of anti-CD47 antibody to be served as a novel promising agent in BTZ-resistant MM.

Ethical approval

All animal works were approved by the Ethics Committee of The Third Affiliated Hospital of Soochow University. All of the procedures were performed in compliance with the Animal Care and Use Regulations of China. Before the specimen collection, written informed consent was obtained, which is not publicly available since the database is not anonymous and contains the patient's name.

Author contributions

Y.H.Y., Y.H.H., and **W.Y.G.** designed the experiments. **Y.H.Y., F.L., Y.T.G., Y.L.**, and **W.M.D.** collected clinical samples. **Y.H.Y., Y.C., N.D. Z., Z.W.Q., X.Y.M.**, and **S.X.G.** conducted the experiments. **Y.H.Y., Y. C.**, and **F.W.** analyzed the data and generated the figures. **Y.H.Y.** and **Y. H.H.** wrote the manuscript. **Y.H.H.** and **W.Y.G.** supervised the project. All authors read and approved the final manuscript.

Conflict of interest

The authors declare that they have no competing interests.

Data availability

All data generated or analyzed during this study are included in this article.

Acknowledgements

This work was partly funded by the key project of Jiangsu Provincial Health Commission (NO. ZD2021043), Changzhou Sci&Tech Program (No. CJ20210075), the Guiding Project of Changzhou Health Bureau (NO. WZ201708), and the Collaborative Innovation Center of Hematology, and the Priority Academic Program Development of Jiangsu Higher Education Institutions. The authors would like to thank Peng Fan and Long Qian (all from Soochow University) for their technical supports.

References

[1] R.L. Siegel, K.D. Miller, A. Jemal, Cancer statistics, 2019, CA Cancer J. Clin. 69 (1) (2019) 7–34.
[2] H.L. Matlung, K. Szilagyi, N.A. Barclay, T.K. van den Berg, The CD47-SIRPα signaling axis as an innate immune checkpoint in cancer, Immunol. Rev. 276 (1) (2017) 145–164.
[3] R. Majeti, M.P. Chao, A.A. Alizadeh, W.W. Pang, S. Jaiswal, K.D. Gibbs Jr., N. van Rooijen, I.L. Weissman, CD47 is an adverse prognostic factor and therapeutic antibody target on human acute myeloid leukemia stem cells, Cell 138 (2) (2009) 286–299.
[4] M.P. Chao, C. Tang, R.K. Pachynski, R. Chin, R. Majeti, I.L. Weissman, Extranodal dissemination of non-Hodgkin lymphoma requires CD47 and is inhibited by anti-CD47 antibody therapy, Blood 118 (18) (2011) 4890–4901.
[5] M. Shi, Y. Gu, K. Jin, H. Fang, Y. Chen, Y. Cao, X. Liu, K. Lv, X. He, C. Lin, H. Liu, H. Li, H. He, J. Qin, R. Li, H. Zhang, W. Zhang, CD47 expression in gastric cancer clinical correlates and association with macrophage infiltration, Cancer Immunol., Immunother. CII 70 (7) (2021) 1831–1840.

[6] R. Imam, Q. Chang, M. Black, C. Yu, W. Cao, CD47 expression and CD163(+) macrophages correlated with prognosis of pancreatic neuroendocrine tumor, BMC Cancer 21 (1) (2021) 320.
[7] O. Arrieta, A. Aviles-Salas, M. Orozco-Morales, N. Hernández-Pedro, A.F. Cardona, L. Cabrera-Miranda, P. Barrios-Bernal, G. Soca-Chafre, G. Cruz-Rico, M.L. Peña-Torres, G. Moncada-Claudio, L.A. Ramirez-Tirado, Association between CD47 expression, clinical characteristics and prognosis in patients with advanced non-small cell lung cancer, Cancer Med. 9 (7) (2020) 2390–2402.
[8] A.A. Barkal, K. Weiskopf, K.S. Kao, S.R. Gordon, B. Rosental, Y.Y. Yiu, B.M. George, M. Markovic, N.G. Ring, J.M. Tsai, K.M. McKenna, P.Y. Ho, R.Z. Cheng, J.Y. Chen, L.J. Barkal, A.M. Ring, I.L. Weissman, R.L. Maute, Engagement of MHC class I by the inhibitory receptor LILRB1 suppresses macrophages and is a target of cancer immunotherapy, Nat. Immunol. 19 (1) (2018) 76–84.
[9] S.R. Gordon, R.L. Maute, B.W. Dulken, G. Hutter, B.M. George, M.N. McCracken, R. Gupta, J.M. Tsai, R. Sinha, D. Corey, A.M. Ring, A.J. Connolly, I.L. Weissman, PD-1 expression by tumour-associated macrophages inhibits phagocytosis and tumour immunity, Nature 545 (7655) (2017) 495–499.
[10] A.A. Barkal, R.E. Brewer, M. Markovic, M. Kowarsky, S.A. Barkal, B.W. Zaro, V. Krishnan, J. Hatakeyama, O. Dorigo, L.J. Barkal, I.L. Weissman, CD24 signalling through macrophage Siglec-10 is a target for cancer immunotherapy, Nature 572 (7769) (2019) 392–396.
[11] M.P. Chao, S. Jaiswal, R. Weissman-Tsukamoto, A.A. Alizadeh, A.J. Gentles, J. Volkmer, K. Weiskopf, S.B. Willingham, T. Raveh, C.Y. Park, R. Majeti, I. L. Weissman, Calreticulin is the dominant pro-phagocytic signal on multiple human cancers and is counterbalanced by CD47, Sci. Transl. Med. 2 (63) (2010) 63ra94.
[12] J. Sun, B. Muz, K. Alhallak, M. Markovic, S. Gurley, Z. Wang, N. Guenthner, K. Wasden, M. Fiala, J. King, D. Kohnen, N.N. Salama, R. Vij, A.K. Azab, Targeting CD47 as a novel immunotherapy for multiple myeloma, Cancers 12 (2) (2020).
[13] J.M. Rendtlew Danielsen, L.M. Knudsen, I.M. Dahl, M. Lodahl, T. Rasmussen, Dysregulation of CD47 and the ligands thrombospondin 1 and 2 in multiple myeloma, Br. J. Haematol. 138 (6) (2007) 756–760.
[14] D. Kim, J. Wang, S.B. Willingham, R. Martin, G. Wernig, I.L. Weissman, Anti-CD47 antibodies promote phagocytosis and inhibit the growth of human myeloma cells, Leukemia 26 (12) (2012) 2538–2545.
[15] F. Zhan, J. Hardin, B. Kordsmeier, K. Bumm, M. Zheng, E. Tian, R. Sanderson, Y. Yang, C. Wilson, M. Zangari, E. Anaissie, C. Morris, F. Muwalla, F. van Rhee, A. Fassas, J. Crowley, G. Tricot, B. Barlogie, J. Shaughnessy Jr., Global gene expression profiling of multiple myeloma, monoclonal gammopathy of undetermined significance, and normal bone marrow plasma cells, Blood 99 (5) (2002) 1745–1757.
[16] N. Rastgoo, J. Wu, A. Liu, M. Pourabdollah, E.G. Atenafu, D. Reece, W. Chen, H. Chang, Targeting CD47/TNFAIP8 by miR-155 overcomes drug resistance and inhibits tumor growth through induction of phagocytosis and apoptosis in multiple myeloma, Haematologica 105 (12) (2020) 2813–2823.
[17] E. Eladl, R. Tremblay-LeMay, N. Rastgoo, R. Musani, W. Chen, A. Liu, H. Chang, Role of CD47 in hematological malignancies, J. Hematol. Oncol. 13 (1) (2020) 96.
[18] Z. Jiang, H. Sun, J. Yu, W. Tian, Y. Song, Targeting CD47 for cancer immunotherapy, J. Hematol. Oncol. 14 (1) (2021) 180.
[19 J. Sun, Y. Chen, B. Lubben, O. Adebayo, B. Muz, A.K. Azab, CD47-targeting antibodies as a novel therapeutic strategy in hematologic malignancies, Leuk. Res. Rep. 16 (2021), 100268.
[20] A. Russ, A.B. Hua, W.R. Montfort, B. Rahman, I.B. Riaz, M.U. Khalid, J.S. Carew, S. T. Nawrocki, D. Persky, F. Anwer, Blocking "don't eat me" signal of CD47-SIRPα in hematological malignancies, an in-depth review, Blood Rev. 32 (6) (2018) 480–489.
[21] X. Liu, Y. Pu, K. Cron, L. Deng, J. Kline, W.A. Frazier, H. Xu, H. Peng, Y.X. Fu, M. M. Xu, CD47 blockade triggers T cell-mediated destruction of immunogenic tumors, Nat. Med. 21 (10) (2015) 1209–1215.
[22] M.O. Peluso, A. Adam, C.M. Armet, L. Zhang, R.W. O'Connor, B.H. Lee, A.C. Lake, E. Normant, S.C. Chappel, J.A. Hill, V.J. Palombella, P.M. Holland, A.M. Paterson, The Fully human anti-CD47 antibody SRF231 exerts dual-mechanism antitumor activity via engagement of the activating receptor CD32a, J. Immunother. Cancer 8 (1) (2020).
[23] Y. Kikuchi, S. Uno, Y. Kinoshita, Y. Yoshimura, S. Iida, Y. Wakahara, M. Tsuchiya, H. Yamada-Okabe, N. Fukushima, Apoptosis inducing bivalent single-chain antibody fragments against CD47 showed antitumor potency for multiple myeloma, Leuk. Res. 29 (4) (2005) 445–450.
[24] J. Laubach, L. Garderet, A. Mahindra, G. Gahrton, J. Caers, O. Sezer, P. Voorhees, X. Leleu, H.E. Johnsen, M. Streetly, A. Jurczyszyn, H. Ludwig, U.H. Mellqvist, W. J. Chng, L. Pilarski, H. Einsele, J. Hou, I. Turesson, E. Zamagni, C.S. Chim, A. Mazumder, J. Westin, J. Lu, T. Reiman, S. Kristinsson, D. Joshua, M. Roussel, P. O'Gorman, E. Terpos, P. McCarthy, M. Dimopoulos, P. Moreau, R.Z. Orlowski, J. S. Miguel, K.C. Anderson, A. Palumbo, S. Kumar, V. Rajkumar, B. Durie, P. G. Richardson, Management of relapsed multiple myeloma: recommendations of the International Myeloma Working Group, Leukemia 30 (5) (2016) 1005–1017.
[25] N. Zhang, R. Yin, P. Zhou, X. Liu, P. Fan, L. Qian, L. Dong, C. Zhang, X. Zheng, S. Deng, J. Kuai, Z. Liu, W. Jiang, X. Wang, D. Wu, Y. Huang, DLL1 orchestrates CD8(+) T cells to induce long-term vascular normalization and tumor regression, Proc. Natl. Acad. Sci. USA 118 (22) (2021).
[26] L. Santo, T. Hideshima, A.L. Kung, J.C. Tseng, D. Tamang, M. Yang, M. Jarpe, J. H. van Duzer, R. Mazitschek, W.C. Ogier, D. Cirstea, S. Rodig, H. Eda, T. Scullen, M. Canavese, J. Bradner, K.C. Anderson, S.S. Jones, N. Raje, Preclinical activity, pharmacodynamic, and pharmacokinetic properties of a selective HDAC6 inhibitor, ACY-1215, in combination with bortezomib in multiple myeloma, Blood 119 (11) (2012) 2579–2589.
[27] L. Zhou, Y. Zhang, Y. Leng, Y. Dai, M. Kmieciak, L. Kramer, K. Sharma, Y. Wang, W. Craun, S. Grant, The IAP antagonist birinapant potentiates bortezomib anti-myeloma activity in vitro and in vivo, J. Hematol. Oncol. 12 (1) (2019) 25.
[28] M.L. Johansen, E.J. Brown, Dual regulation of SIRPalpha phosphorylation by integrins and CD47, J. Biol. Chem. 282 (33) (2007) 24219–24230.
[29] M. Locati, G. Curtale, A. Mantovani, Diversity, mechanisms, and significance of macrophage plasticity, Annu. Rev. Pathol. 15 (2020) 123–147.
[30] B.Z. Qian, J.W. Pollard, Macrophage diversity enhances tumor progression and metastasis, Cell 141 (1) (2010) 39–51.
[31] A. Zumsteg, G. Christofori, Corrupt policemen: inflammatory cells promote tumor angiogenesis, Curr. Opin. Oncol. 21 (1) (2009) 60–70.
[32] J. Sun, C. Park, N. Guenthner, S. Gurley, L. Zhang, B. Lubben, O. Adebayo, H. Bash, Y. Chen, M. Maksimos, B. Muz, A.K. Azab, Tumor-associated macrophages in multiple myeloma: advances in biology and therapy, J. Immunother. Cancer 10 (4) (2022).
[33] A. Calcinotto, M. Ponzoni, R. Ria, M. Grioni, E. Cattaneo, I. Villa, M.T. Sabrina Bertilaccio, M. Chesi, A. Rubinacci, G. Tonon, P.L. Bergsagel, A. Vacca, M. Bellone, Modifications of the mouse bone marrow microenvironment favor angiogenesis and correlate with disease progression from asymptomatic to symptomatic multiple myeloma, Oncoimmunology 4 (6) (2015), e1008850.
[34] C.S. Chim, S.K. Kumar, R.Z. Orlowski, G. Cook, P.G. Richardson, M.A. Gertz, S. Giralt, M.V. Mateos, X. Leleu, K.C. Anderson, Management of relapsed and refractory multiple myeloma: novel agents, antibodies, immunotherapies and beyond, Leukemia 32 (2) (2018) 252–262.
[35] N. Lehners, N. Becker, A. Benner, M. Pritsch, M. Löpprich, E.K. Mai, J. Hillengass, H. Goldschmidt, M.S. Raab, Analysis of long-term survival in multiple myeloma after first-line autologous stem cell transplantation: impact of clinical risk factors and sustained response, Cancer Med. 7 (2) (2018) 307–316.
[36] S.M. Ansell, M.B. Maris, A.M. Lesokhin, R.W. Chen, I.W. Flinn, A. Sawas, M. D. Minden, D. Villa, M.M. Percival, A.S. Advani, J.M. Foran, S.M. Horwitz, M. G. Mei, J. Zain, K.J. Savage, C. Querfeld, O.E. Akilov, L.D.S. Johnson, T. Catalano, P.S. Petrova, R.A. Uger, E.L. Sievers, A. Milea, K. Roberge, Y. Shou, O.A. O'Connor, Phase I Study of the CD47 Blocker TTI-621 in patients with relapsed or refractory hematologic malignancies, Clin. Cancer Res. 27 (8) (2021) 2190–2199.
[37] J. Lin, W. Zhang, J.J. Zhao, A.H. Kwart, C. Yang, D. Ma, X. Ren, Y.T. Tai, K. C. Anderson, R.I. Handin, N.C. Munshi, A clinically relevant in vivo zebrafish model of human multiple myeloma to study preclinical therapeutic efficacy, Blood 128 (2) (2016) 249–252.
[38] Y. Zheng, Z. Cai, S. Wang, X. Zhang, J. Qian, S. Hong, H. Li, M. Wang, J. Yang, Q. Yi, Macrophages are an abundant component of myeloma microenvironment and protect myeloma cells from chemotherapy drug-induced apoptosis, Blood 114 (17) (2009) 3625–3628.
[39] M. Sun, S. Qiu, Q. Xiao, T. Wang, X. Tian, C. Chen, X. Wang, J. Han, H. Zheng, Y. Shou, K. Chen, Synergistic effects of multiple myeloma cells and tumor-associated macrophages on vascular endothelial cells in vitro, Med. Oncol. 37 (11) (2020) 99.
[40] N. Jetten, S. Verbruggen, M.J. Gijbels, M.J. Post, M.P. De Winther, M.M. Donners, Anti-inflammatory M2, but not pro-inflammatory M1 macrophages promote angiogenesis in vivo, Angiogenesis 17 (1) (2014) 109–118.
[41] R.K. Jain, Normalization of tumor vasculature: an emerging concept in antiangiogenic therapy, Science 307 (5706) (2005) 58–62.
[42] S.K. Martin, A.L. Dewar, A.N. Farrugia, N. Horvath, S. Gronthos, L.B. To, A. C. Zannettino, Tumor angiogenesis is associated with plasma levels of stromal-derived factor-1alpha in patients with multiple myeloma, Clin. Cancer Res. 12 (23) (2006) 6973–6977.
[43] F. Di Raimondo, M.P. Azzaro, G. Palumbo, S. Bagnato, G. Giustolisi, P. Floridia, G. Sortino, R. Giustolisi, Angiogenic factors in multiple myeloma: higher levels in bone marrow than in peripheral blood, Haematologica 85 (8) (2000) 800–805.
[44] M. De Palma, D. Biziato, T.V. Petrova, Microenvironmental regulation of tumour angiogenesis, Nat. Rev. Cancer 17 (8) (2017) 457–474.
[45] R. Hughes, B.Z. Qian, C. Rowan, M. Muthana, I. Keklikoglou, O.C. Olson, S. Tazzyman, S. Danson, C. Addison, M. Clemons, A.M. Gonzalez-Angulo, J. A. Joyce, M. De Palma, J.W. Pollard, C.E. Lewis, Perivascular M2 macrophages stimulate tumor relapse after chemotherapy, Cancer Res. 75 (17) (2015) 3479–3491.
[46] Q. Wang, G.E. Lash, Angiopoietin 2 in placentation and tumor biology: the yin and yang of vascular biology, Placenta 56 (2017) 73–78.
[47] R. Mazzieri, F. Pucci, D. Moi, E. Zonari, A. Ranghetti, A. Berti, L.S. Politi, B. Gentner, J.L. Brown, L. Naldini, M. De Palma, Targeting the ANG2/TIE2 axis inhibits tumor growth and metastasis by impairing angiogenesis and disabling rebounds of proangiogenic myeloid cells, Cancer Cell 19 (4) (2011) 512–526.
[48] S. Kaur, S.M. Bronson, D. Pal-Nath, T.W. Miller, D.R. Soto-Pantoja, D.D. Roberts, Functions of thrombospondin-1 in the tumor microenvironment, Int. J. Mol. Sci. 22 (9) (2021).
[49] A. Bikfalvi, Platelet factor 4: an inhibitor of angiogenesis, Semin. Thromb. Hemost. 30 (3) (2004) 379–385.
[50] T. Kammertoens, C. Friese, A. Arina, C. Idel, D. Briesemeister, M. Rothe, A. Ivanov, A. Szymborska, G. Patone, S. Kunz, D. Sommermeyer, B. Engels, M. Leisegang, A. Textor, H.J. Fehling, M. Fruttiger, M. Lohoff, A. Herrmann, H. Yu, R. Weichselbaum, W. Uckert, N. Hübner, H. Gerhardt, D. Beule, H. Schreiber, T. Blankenstein, Tumour ischaemia by interferon-γ resembles physiological blood vessel regression, Nature 545 (7652) (2017) 98–102.